

# Spectral Analysis of SN1987A

P. Höflich and J. C. Wheeler

*Astronomy Department, University of Texas, Austin, TX 78712*

**Abstract.** We examine the current status of the spectral analysis of SN1987A during its early stages. Issues of the shock breakout and UV flash, the density and chemical structure, and masses of different layers are discussed. A decade later, several aspects need a fresh look and interpretation. We summarize what questions have been answered and where some results disagree. Unresolved problems such as the excess of s-process elements and influence of asphericity are addressed. Finally, SN1987A is considered as a test case for using Type II as distance indicators via the Baade-Wesselink method.

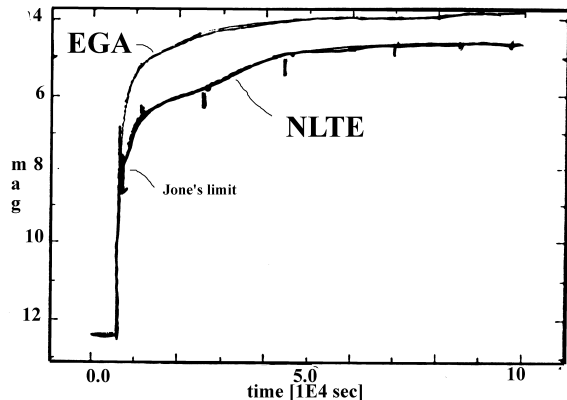
## 1. Introduction

The emitted light of Type II supernovae allows study of the explosion mechanism, testing of hydrodynamic models and probing of the final stages of the stellar evolution. The observed spectrum gives direct information on the physical and chemical conditions of the supernova photosphere at a given time. Deeper layers are observable at later times. Spectral analysis provides an effective tool to scan through the atmosphere, to reveal the density, chemical, and velocity structure, to probe explosion models, to reveal mixing processes and departures from sphericity, and to determine the distance. At any one time, the photosphere spans only about  $10^{-4}$  to  $10^{-2}M_{\odot}$  and, consequently, good time coverage is critical to derive integrated quantities such as the total mass. The following analysis is mainly based on our own work but, for comparison, we will refer to results of other groups as appropriate (Table 1). Specific references are given in the text.

Table 1. Some Work on Atmosphere Models of SN 1987A

First Authors	Phase	Topic
Ensmann/Hauschildt	0-4 d	shock breakout, early spectra + colors
Höflich	0-220d	shock breakout, abundances, structure, mixing, asphericities, CO, distance
Lucy/Mazzali	2-100d	structure + abundances
Jeffery	2-30d	asphericity
Eastman	2-10d	structure/distance by Baade-Wesselink
Schwarz	150-500d	gamma excitation
Li/McCray	200+d	gamma excitation, mixing
Wagoner/Chilukuri	2-50 d	distance by Baade-Wesselink

Figure 1. Observed  $m_V$  (with measurement error bars) of SN1987A in comparison with that predicted by a model with  $1.25 \times 10^{51}$  erg (Shigeyama & Nomoto, 1990) using NLTE and extended grey atmospheres (EGA). The distance is taken to be 48 kpc.  $E_{B-V}$  is set to  $0.15^m$ .



## 2. Model Assumptions and Free Parameters

Most of the calculations summarized here were performed prior to 1989 and, consequently, the description of our Nlte code for Extended ATmospheres (NEAT) below corresponds to this era (Höflich 88ab, 90, 91a; hereafter H stands for Höflich). It has since been updated. The system of equations and their solution is briefly described as follows. a) The radiation transport equation is solved in the comoving frame and includes relativistic velocity fields and line blanketing (Mihalas et al., 1975, 76ab). Time dependent terms can be neglected because the radiative time scales are short compared to those of physical quantities at the photosphere. b) The statistical equations are solved by a perturbation method (ALI). For the early light curve (LC), time dependent statistical equations are solved (H91a). c) The energy equation. During later phases, we assume homologous expansion and radiative equilibrium to determine the thermal structure. The bolometric and  $\gamma$ -ray luminosities are taken from the observations. The  $\gamma$ -ray energy deposition is treated following Colgate et al. (1980). During the shock breakout, the temperature structure is taken from the hydro because it is governed by adiabatic expansion and the corresponding recession in mass of the photosphere (see also Hauschildt & Ensmann 1994, hereafter HE94). Detailed atomic models are used for up to the three most abundant ionization stages of several elements (H, He, C, N, O, Na, Mg, K, Ca). A large number of LTE-lines is included in a pure scattering approximation.

## 3. The Shock Breakout

SN1987A is the first Type II supernova to have been observed shortly after the initial event (e.g. McNaught 1987). Measurements of the envelope mass and explosion energy based on the early LC are consistent with the interpretation of the late LC (Arnett, 1988; Nomoto et al., 1988; Woosley, 1988); however, flux limited diffusion calculations gave discrepancies between observations and models of up to 2 magnitudes at the earliest phases.

To address this problem, H91a coupled the hydrodynamical calculations of Shigeyama & Nomoto (1990) with a detailed atmosphere. The progenitor has a total mass of  $16 M_{\odot}$ ,  $10.4 M_{\odot}$  of H, a radius  $R_{ph} = 3 \times 10^{12}$  cm. Explosions

have been investigated with  $E_{kin}$  of  $1.0 \times 10^{51}$  and  $1.25 \times 10^{51}$  erg which give a reasonable reproduction of the late light curve. Both NLTE and scattering effects are important (Fig. 1, Höflich et al., 1986, H90, H91a, Pizzochero, 1990). The NLTE fluxes differ from those resulting from a flux limited diffusion approach or the solution for an extended gray atmosphere (EGA), and the slope of the LC changes. In particular,  $L_V$  shows a strong local minimum shortly after shock break out. The general tendencies, and the drop in  $L_V$ , can be understood as a consequence of the rapid drop in  $\rho$  and  $T$  and the resulting size of NLTE effects and of the scattering optical depth (H91a).

Table 2 gives the results of NLTE atmosphere models during the shock breakout phase; the electron temperature  $T$ , the radius of the photosphere  $R$ , the particle density  $N_o$  (in cgs) at the Thomson optical depth of  $2/3$ ,  $M_V$ , U-B, B-V and the bolometric luminosity  $L_{bol}$  based on the hydrodynamic calculation of Shigeyama & Nomoto (1990). The dynamical model had logarithmic zoning that resolved the photosphere at the epoch of the Jones' limit. The functions  $C_V$  and  $C_{bol}$  give the ratio of the visual and bolometric fluxes, respectively, calculated by NLTE models to those of the extended grey atmosphere (EGA). Observed colors are in good agreement ( $t=4.4 \times 10^4$  s B-V=-0.2 ... 0.0; at  $9.83 \times 10^4$  s U-B=-0.836, B-V=0.085, Moreno & Walker 1987).

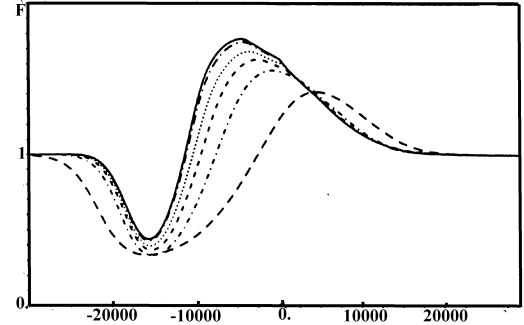
Table 2. Results of NLTE calculations of Shock Breakout

time [s]	T[K]	R	$N_o$	$M_V$	U-B	B-V	$L_{bol}$	$C_V$	$C_{bol}$
6175.	788000.	3.36E12	6.3E14	-11.75	-1.23	-0.30	4.6E44	0.18	0.39
6400.	399450.	4.20E12	7.8E13	-10.99	-1.28	-0.32	8.7E43	0.13	0.32
7000.	282000.	6.28E12	3.2E13	-11.19	-1.33	-0.33	5.0E43	0.12	0.28
8000.	102000.	9.56E12	1.1E13	-11.46	-1.23	-0.28	8.5E42	0.19	0.24
10791.	56200.	1.90E13	5.2E11	-12.45	-1.20	-0.29	9.2E41	0.21	0.22
26411.	27000.	5.44E13	1.8E11	-13.21	-1.02	-0.24	1.6E41	0.23	0.30
44974.	18700.	8.92E13	9.8E10	-14.16	-0.98	-0.22	1.2E41	0.30	0.36
70104.	14900.	1.28E14	7.5E10	-14.36	-0.95	-0.14	8.5E40	0.33	0.38
99892.	12100.	1.70E14	5.0E10	-14.46	-0.82	-0.07	8.3E40	0.37	0.43

The explosion energy  $E_{kin}$  is not well determined by the absolute visual flux because of uncertainties in the distance and measurements, but can be estimated rather precisely by the rise time and the location of the first local minimum in V that depend on the shock travel time. Assuming that the time of the initial core collapse is given by the neutrino detections, a value of  $E_{kin} = 1.0 \times 10^{51}$  erg can be ruled out. Since the shock travel time through the progenitor is essentially proportional to  $E_{kin}^{0.5}$ , the energy must be larger than  $1.20 \times 10^{51}$  erg. A value  $E_{kin} = 1.25 \times 10^{51}$  erg leads to a good agreement with the observations. Another, less stringent, upper limit can be derived from the upper limit set by Jones. SN1987A would have been seen by Jones if the shock travel time were about 30 minutes shorter. Therefore,  $E_{kin}$  must be  $\leq 1.6 \times 10^{51}$  erg. The hard UV fluxes are consistent with the observed high excitation lines of NV and OVI in the circumstellar ring (Fransson & Lundqvist, 1989).

In the calculations just described no correction to the original temperature distribution given by flux-limited diffusion was made for the NLTE radiation field. This limitation was addressed by Mair et al. (1992) who used a gray radiation hydro code with adaptive mesh. For Arnett's  $15 M_\odot$  model, Mair et

Figure 2.  $H_\alpha$  profiles with  $v_{stat}/v(R_{ph})$  [in %] of 0 (solid), 1 (long dashed-dotted), 5 (dotted), 10 (short dashed), 20 (short dashed dotted) and 50 (long dashed) for a parameterized model with  $T_{eff} = 10,000$  K,  $R_{ph} = 1.3 \times 10^{15}$  cm,  $v(R_{ph}) = 10,000$  km s $^{-1}$  and  $\rho \propto r^{-7}$  (Duschinger et al. 1995).



al. found that  $E_{kin}$  must be close to  $1.3 \times 10^{51}$  erg and excluded  $1.0 \times 10^{51}$  erg. Ensmann & Burrows (1992) and HE94 analyzed the explosion of Arnett's  $17 M_\odot$  model with an explosion energy of  $1.0 \times 10^{51}$  erg. These analyses are similar to the approach just described using a combination of a gray radiation hydro code and NLTE-atmospheres (without time dependence). The explosion was followed up to day 4. As also stated in HE94, a problem seems to be that the photosphere recedes too rapidly and, consequently, the Doppler shifts of the absorption lines are too low after about day two. This suggests that a larger value of  $E_{kin}$  is required, as concluded above.

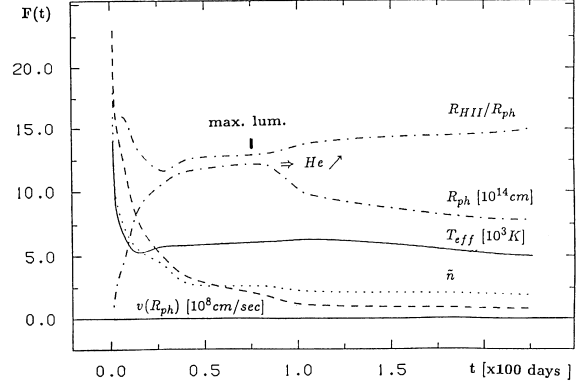
#### 4. The Photospheric Phase

A variety of structures for the later photospheric phase were tested (e.g. H87, H88ab), based on explosions of models with a main sequence masses between 15 to  $20 M_\odot$  provided by Weiß(private communication). The best agreement was found for  $18 M_\odot$ . A statistical velocity field  $v_{stat}$  was introduced to improve the agreement between observed and calculated spectra. The size of  $v_{stat}$  is small in comparison to  $v_{exp}$  but larger than the sound speed,  $\approx 15\%$  of  $v_{exp}$  during the first week and  $5\%$  thereafter. This quantity should not be interpreted as microturbulence, but as a velocity field with a scale height smaller than the free mean path of the line photons (H87, H88a, see §6). With increasing  $v_{stat}$ , the features become broader, the emission component is more red shifted and the rise from the minima to the maxima of the P-Cygni profile is slower (Fig. 2).

The luminosity was taken to be proportional to the observed bolometric LC. The choice of  $E_{kin}$  and the distance then determines the time evolution of the photospheric parameters such as  $R_{ph}$ ,  $T_{eff}$ , the radius  $R_{HII}$  of the outer boundary of the ionized hydrogen region, and the matter velocity at the photosphere (see Fig. 3). The spectral evolution and the colors are well reproduced as shown in Figures 4 and 5 (H87, H88ab). Spectral analysis of the photospheric phase gives  $E_{kin} = 1.3 \times 10^{51}$  erg, consistent with the shock break out and early LC analysis. The distance is discussed in §5.

The difference between the spectral evolution of SN1987A and most other SN II can be understood as a consequence of the compact structure of the progenitor star which implies higher densities and steeper density gradients, and a

Figure 3. Distance  $R_{ph}$ ,  $T_{eff}$ , velocity  $v$  at  $R_{ph}$ , the power law index  $\tilde{n}$  of the corresponding power law density slope and the distance  $R_{HII}$  up to which hydrogen is mainly ionized are given as a function of time.



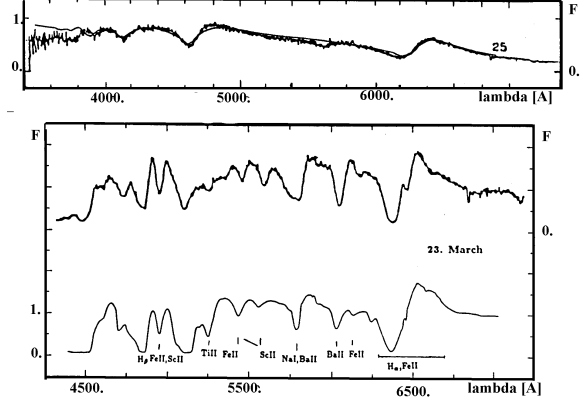
low total luminosity. For SN1987A, the recombination phase of the photosphere is encountered already after about 1 to 2 weeks.

Early on, the location of  $R_{ph}$  is strongly coupled to the expanding matter due to the high temperature and density at the photosphere. Consequently, the effective temperature  $T_{eff}$  drops very rapidly in the presence of a slowly varying total luminosity. This causes the rapid variations of the continuum flux in the UV, optical and IR during the first week. The smaller changes in the following months are due to the slow increase of  $R_{ph}$ , due mainly to a geometrical dilution effect and to the recombination of H outside the radius  $R_{HII}$ . The decrease of  $R_{ph}$  after maximum light is caused by the decreasing luminosity and by the higher helium abundances. Helium is mainly neutral and does not contribute to the electron density at the photosphere. Thus, the increase of the color temperature after maximum light is mainly a result of the increased helium abundance. The IR-excess can be understood as owing to free-free radiation and extension effects ( $\approx 10$  to  $20$  %). No additional dust component is needed during the first few months at least in the nearer IR (H88ab).

The observed frequency shifts of the absorption components of the Balmer lines are formed at different depths and hence probe the  $v/\rho$  structure (H91b). The good agreement between observed and calculated line shifts confirms the density profiles  $\rho(r)$ . Lucy (1987) found similar density gradients from his analyses which are mainly based on the UV spectra. HE94 show fits of similar quality during the first 3 days with more self-consistent models (i.e. they calculate the luminosity from the radiation-hydro calculation). Their assumed  $\rho(r)$  is consistent with H87, H88, H91ab. At  $t=2d$ :  $\rho(R_{ph}) \propto r^{-9}$  vs.  $\propto r^{-10}$  in our work. Both in H87 and HE94 the  $\rho$  gradient changes over the line forming region by  $\approx 20$  %. Eastman & Kirshner (1989) used  $R_{ph}$ ,  $T_{eff}$  and  $\rho(r) \propto r^{-\tilde{n}}$  as free parameters at each time. Although unrealistic, they used constant power law density profiles. They find gradients consistent with those given above ( $\tilde{n}(t=2d) = 9$ ;  $\tilde{n}(t=10d) = 5$  to  $7$  vs.  $10$  and  $7.2$ , respectively in H87).

After one to two weeks, the Thomson scattering opacity declines due to recombination and heavy elements appear because weak lines are no longer “washed out.” This spectral change does not imply a change in the composition. Abundances less than solar are needed in order to reduce line blanketing by the metal lines. The abundances must be about one third of solar for nearly all elements (H88ab). This value closely resembles that derived for the LMC by

Figure 4. Spectra as observed by Menzies et al. (1987) February 25.9 and March 23rd, 1987, in comparison with the synthetic spectra.

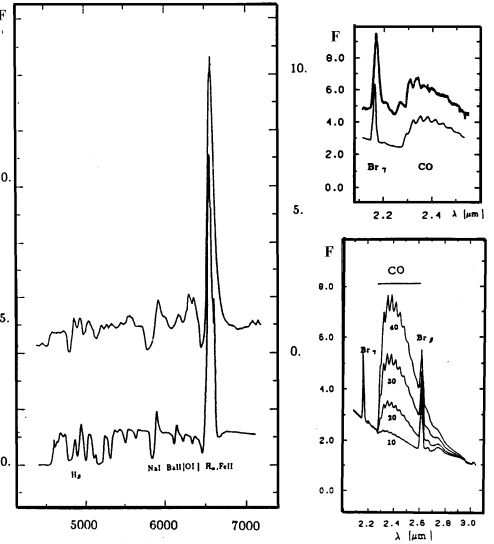


Dufour (1984). The exception in SN 1987A is the s-process elements Sc, Ti, V, Cr, Sr, Ba and Na. An overabundance relative to solar of Sc, V, Cr, Sr and Ti is needed to explain the slope of the spectrum below 5300 Å. The strong line at about 6100 Å can be attributed to Ba II (Williams 1988, H88ab) if Ba is increased by about 8-10 relative to LMC abundances. Other BaII features are present in the observed and calculated spectra at about 4900 Å and 5000 Å. They are consistent with the same overabundance; however blanketing by other lines prohibits a detailed analysis. Using Lucy's Monte Carlo code, Mazzali & Chugai (1995) reanalyzed the spectra and found an overabundance for Ba of about 4 which is consistent within the uncertainties with other analyses.

The evolving spectra are well reproduced by the atmosphere models during the first 5 months; however, later spectra (i.e. June, H88a) show insufficient blue shifts indicating too small a photospheric velocity. A power law density profile was introduced that yielded higher central densities than the original dynamical model. This is a crude way to allow for the entropy redistribution that must accompany mixing. At this epoch, excitation by  $\gamma$ -rays must also be taken into account because it strongly influences the temperature and ionization structure. The size of the  $\gamma$ -ray flux is assumed to be that given by the SMM satellite (Gehrels et al. 1989).  $\gamma$ -ray heating and inefficient cooling leads to high temperatures in the outer H-envelope and substantial emission by the cooling lines, e.g. Ca, despite their low abundance (Schwarz 1991, Li & McCray 1996).

The calculated and observed spectrum on October 2 (Fig. 5) are in good agreement, if we choose roughly the same chemical abundances, but enrich He by a factor of 5. This implies that by this phase He-rich layers are seen. From the spectral analysis, the mass of the H-rich envelope is about  $10 M_{\odot}$  (H88ab). A decrease of the H abundance is needed to explain the strong decrease of the continuum flux relative to the lines. The increase in the He abundance leads to a strong decrease of  $R_{ph}$ , since He is mainly neutral. Furthermore, this explains in a consistent way the increase of the color temperature given by B-V. At this time, hydrogen is still seen at the photosphere which shows an expansion velocity of the order of only  $800 \text{ km s}^{-1}$ . At the same time, CO bands in the IR indicate that the matter is strongly enriched with C and O up to radii that correspond to an expansion velocity of the order of  $1800 \text{ km s}^{-1}$ . These results strongly indicate that about  $3M_{\odot}$  of H have been mixed into very deep layers (H88ab; Li et al. 1993) of the ejecta and a moderate mass of C and O-rich matter,  $\sim 10^{-2}$

Figure 5. Synthetic optical and IR spectra corresponding to October 2<sup>nd</sup>, 1987, in comparison with observations in the optical (Oct. 2<sup>nd</sup>, Danziger, priv. comm.; left) and in the IR (ESO observations between 1. and 6. Oct. 1987/shifted by two units, lower right). C and O was assumed to be enhanced to 20 \* solar up to 1800 km/sec. In addition, the theoretical CO spectra are given for various enhancement factors (lower right). Mixing out CO up to 3000 km/sec would produce featureless CO-bands (Sharp & Höflich 1989). The feature at 2.38  $\mu$ m cannot be attributed to  $CO^+$ .

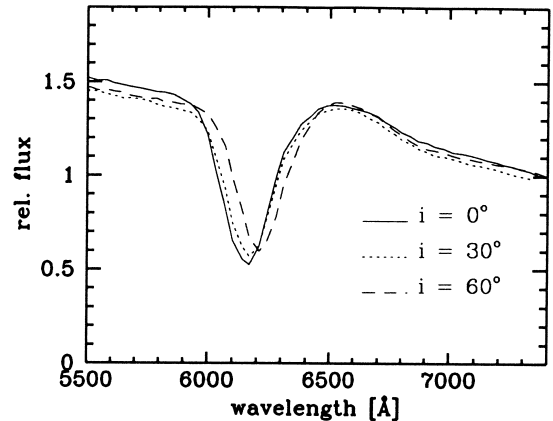


to  $10^{-1}M_{\odot}$  have been mixed far out into the H-rich matter. This mixing can be understood by Rayleigh-Taylor instabilities during the explosion. Mixing was also indicated by the time dependence of the observed hard  $\gamma$ -rays, the detection of broad IR lines of Co and Fe, and the LCs ( e.g. Woosley, 1988).

## 5. Distance to SN1987A

Distances to many SN II have been derived by using the Baade-Wesselink method (e.g. SN 1969L:  $12 \pm 4$  Mpc and SN 1970G:  $7 \pm 2$  Mpc Kirshner & Kwan, 1974; SN1979C:  $23 \pm 3$  Mpc , Branch et al., 1981). In this method the ratios of the observed and predicted fluxes and spectral slopes at different wavelengths together with the velocities at different times are used to derive quantities such as the photospheric radius. In the past, these determinations were based on the assumption that the radiation of the supernova can be represented by a black body; however, the dilution of the radiation field and line blanketing are critical (Höflich et al. 1986, Hershkowitz et al. 1986, H91c, Schmidt et al. 1994, Baron et al. 1995, Eastman et al. 1996). For high temperatures, the dilution factors are rather insensitive to the model parameters (10 to 25 %), but the absolute size given in the literature ranges from  $\approx 0.3$  (Eastman et al. 1996) to 0.5 (Baron et al. 1995) with H91c being somewhere in between. There is general agreement that the dilution factor rises steeply with declining  $T_{eff}$  during the recombination phase of hydrogen (H91d, Schmidt et al. 1994). Typically, this phase is entered a few weeks after the explosion and is accompanied by the appearance of metal lines in the optical spectra. The critical  $T_{eff}$  for the onset of this rise depends sensitively on several parameters such as the structure and the He/H ratio. Unfortunately, uncertainties in the time since the explosion,  $\Delta t$ , enter the distance determination as  $\Delta t/t$ . This, together with the large sensitivity of the dilution factor as a function of T in the relevant range  $\sim 5000$  K, poses a significant limitation on the accuracy of the Baade-Wesselink method; however

Figure 6.  $H_\alpha$  profile for different inclinations  $i$  for an oblate ellipsoid calculated by a 3-D NLTE code. An axis ratio of 0.85 is assumed. Parameters representing the atmosphere of SN1987A at about day 3 after the explosion ( $T_{eff} = 9000$  K,  $R_{ph, \tau_{sc}=1} = 8. \times 10^{14}$  cm,  $\rho \propto r^{-9}$ ). For details, see Höflich et al. (1995) & Wang et al. (1997).



high accuracy can be achieved if a detailed analysis of a broad range of data (including the time of the explosion) can be done. SN1987A can be regarded as the benchmark to demonstrate the “ideal” case. Based on the detailed spectral analysis for the first 200 days, (H88ab) derived a distance of  $48 \pm 4$  kpc, well within the error bars of other groups (e.g. Chilukuri & Wagoner 1988:  $43 \pm 4$  kpc; Schmutz et al. 1990: 46 kpc; Eastman & Kirshner 1989:  $49 \pm 5$  kpc).

## 6. Deviations from Sphericity

For SN1987A, polarization  $P$  of up to 0.5 % was observed early on. The level of  $P$  decreased rapidly over the next few weeks (e.g. Mendez et al. 1988). It was concluded that the envelope of SN1987A showed asphericities of about 10 to 20 % and that Thomson scattering was the mechanism to produce  $P$  (Jeffery, 1991, Mendez et al. 1988, Höflich et al. 1989, H91b). Whether  $P$  is caused by rapid rotation of the progenitor (Steinmetz & Höflich 1992), by an asphericity of the SN II-explosion mechanism (Yamada & Sato 1991), by an asymmetric luminosity input (H95), or dust in the surroundings (Wang & Wheeler 1996) is still a question under debate. There is growing evidence that, whatever the combination of mechanisms, polarization is a rather common phenomenon among SNe II (Wang et al. 1995). The implications for our understanding of the explosion mechanism and progenitor evolution are obvious. There is also a direct impact on the use of SNe II as distance indicators because aspherical configurations also result in aspherical luminosities. An appreciable systematic bias will enter in statistical analyses when many SNe II are used to determine  $H_0$  because the directional redistribution of photons is different from the probability distribution of the inclination angle seen by an observer (H91c). For a more detailed discussion of  $P$  see Wang, Wheeler & Höflich (this volume).

The finite polarization of SN II suggests a possible interpretation of the high statistical velocity deduced for SN 1987A as discussed in §4. An aspherical

configuration has some qualitatively similar effects on the spectra as a statistical velocity because both increase the spread in velocities observed at a given epoch, as can be seen by comparing Figures 2 and 6. Both cause the rise from the minima to the maxima to be less steep and the emission is shifted compared to a spherical configuration without  $v_{stat}$  (not shown in Fig. 6). In spite of the similarity, there does not exist a direct correspondence between the parameters for a spherical configuration  $v_{stat}$  and an aspherical configuration. More studies based on 3-D NLTE atmospheres are required (see Wang et al. 1997 for SNe Ia).

## 7. Conclusions and Open Questions

The peculiarities of the spectral and color evolution of SN1987A can be understood by the fact that the progenitor was a blue supergiant with its compact structure and low luminosity. Both from the early LC and the spectra we can conclude that  $E_{kin}$  is about  $1.3 \times 10^{51} \pm 0.3$  erg based on stellar models with  $R_{ph} = 3.10^{12}$  cm. The hydrogen-rich envelope is about  $9 - 11 M_{\odot}$ . The uncertainty of the total mass of H is relatively small because of the weak dependence of the density at the photosphere on the atmosphere model parameters. Strong mixing of  $3 M_{\odot}$  of H with the inner layers (down to  $800 \text{ km s}^{-1}$ ) and mixing of C/O rich layers out to about  $1800 \text{ km s}^{-1}$  was found. This can be understood by Rayleigh-Taylor instabilities during the explosion, but a full radiative transfer of a self-consistently mixed model has not been done. The metal abundances are consistent with the chemical composition of the LMC, but the s-process elements are highly enriched. The abundance ratios of the s-process elements are in agreement with the s-process (Hashimoto et al. 1990), but the origin of the enhancement remains unexplained. Polarization suggests asphericity in the outer layers of SN1987A of about 10 %. This may explain the high statistical velocity field needed to fine tune spectral fits during early epochs (H87); however, more detailed analysis is needed to test this suggestion.

This research is supported by NSF Grant AST9528110.

## References

- Arnett W.D. 1988, ApJ 331, 377
- Baron E. et al. 1995, ApJ 441, 170
- Branch D. et al. 1981, ApJ 244, 780
- Chilukuri M., Wagoner R.V., 1988, IAU Symposium 108, ed. K. Nomoto, Springer, p. 295
- Colgate S.A., Petschek A.G., Kreise J.T. 1980, ApJ 237, L81
- Dufour R.J. 1984, IAU Colloquium 108, ed. K. Nomoto, Springer, p. 353
- Duschinger M., Puls J., Branch D., Höflich P., Gabler A. 1995 A&A 297, 802
- Eastman R. G., Kirshner R.P. 1989, ApJ 347, 771
- Eastman R. G., Schmidt B.P., Kirshner R.P. 1996, ApJ 466, 911
- Ensmann L., Burrows A. 1992, ApJ 393, 742
- Fransson C., Lundqvist P. 1988, ApJ 341, L59

Gehrels, N., MacCallum C.J., Leventhal M. 1989, ApJ 317, L73  
 Hashimoto M., Nomoto K., Shigeyama T. 1989, A&A 210, L5  
 Hauschildt, P., Ensman L. 1994, ApJ 424, 905  
 Hershkowitz R., Lindner E., Wagoner B. 1986, A&A 301, 220  
 Höflich P., Wehrse R., Shaviv G. 1986, A&A 163, 105  
 Höflich P. 1987, in *SN 1987A*, ed. by I.J. Danziger, ESO, p. 449  
 Höflich P. 1988a, IAU Colloquium 108., ed. K. Nomoto, Springer, p. 288  
 Höflich P. 1988b, PASA 7, 434  
 Höflich P. 1990, Habil. Thesis, U. of Munich, MPA-563  
 Höflich P. 1991a, in *SN 1987A & other SNe*, ed. J. Danziger, ESO, p. 387  
 Höflich P. 1991b, A&A 246, 481  
 Höflich P. 1991c, in “Supernovae”, ed. S.E. Woosley, Springer, p.415  
 Höflich P. et al. 1995, ApJ 459, 307  
 Jeffery D. 1991, ApJ 352, 267  
 Kirshner R., Kwan J., 1974, ApJ 193, 27  
 Li, H., McCray, R. A., and Sunayev, R. A. 1993, ApJ 419, 824  
 Li, H., McCray, R. 1996 ApJ 456, 370  
 Lucy, 1987, in *SN1987A & other SNe*, ed. J. Danziger, ESO, p. 302  
 Mair, G., Hillebrandt, W., Höflich, P., Dorfi, E. A&A 266, 266  
 Mazzali M., Chugai, N. 1995 A&A 303, 118  
 McNaught R. H., 1987 IAU Circular, 4389  
 Mendez M., Clocchiatti A., Benvenuto G., Feinstein C. 1988, ApJ 334, 295  
 Mihalas D., Kunasz R.B., Hummer D.G. 1975, ApJ 202, 465  
 Mihalas D., Kunasz R.B., Hummer D.G. 1976a, ApJ 206, 515  
 Mihalas D., Kunasz R.B., Hummer D.G. 1976b, ApJ 210, 419  
 Moreno B., Walker S., 1987 IAU Circular 4316  
 Nomoto K., Shigeyama T., Kumagai S., Hashimoto S., 1988, PASA 7, 490  
 Pizzochero P. 1991, in *SN1987A & other SNe*, ed. J. Danziger, ESO, p. 203  
 Schmidt B.P. et al. 1994, ApJ 432, 42  
 Schmutz W. et al 1990, ApJ 355, 255  
 Schwarz D. 1991, in “Supernovae”, ed. S.E. Woosley, Springer, p. 437  
 Sharp C., Höflich P. 1989, Astr.Sp.Sc. 171, 213  
 Shigeyama T., Nomoto K. 1990, ApJ 360, 242  
 Steinmetz M., Höflich P. 1991, A&A 257, 641  
 Wang L., Wheeler J.C., Li, Z.W., Clocchiatti, A. 1996, ApJ 467, 435  
 Wang L., Wheeler J.C. 1996, ApJ, 462, L27  
 Wang L., Wheeler J.C., Höflich, P. 1997, ApJ 476, L27  
 Williams R.E. 1988, 4th George Mason Conf., ed.M. Kafatos, p. 355  
 Woosley S.E. 1988, IAU Colloquium 108, ed. K. Nomoto, Springer, p. 361  
 Yamada, S.; Sato, K., 1990, ApJ 358, L9